scientific reports

Check for updates

OPEN

A bispecific anti-MUC16/anti-death receptor 5 antibody achieves effective and tumor-selective death receptor 5-mediated tumor regression

Victor S. Goldmacher✉, Iosif Gershteyn, Ravi Chari & Yelena Kovtun

The bispecific antibody IMV-M was designed to selectively bind and cluster death receptor 5 (DR5) upon engaging the tumor antigen MUC16 through a novel mechanism—clustering multiple IMV-M molecules on a single MUC16 molecule. IMV-M demonstrated potent, MUC16-selective anti-tumor activity in vitro and in xenograft models without requiring secondary crosslinking, and a pilot non-human primate toxicity study detected no toxicity. Our findings suggest that antibody clustering effectively induces DR5 clustering, resulting in anti-tumor activity. Unlike anti-MUC16 antibody-drug conjugates (ADCs), which rely on cytotoxic payloads, this approach offers a safer and more effective therapeutic strategy. Notably, MUC16 is overexpressed in substantial subsets of ovarian, pancreatic, and lung cancers, with minimal expression in normal tissues, suggesting the broad applicability of this bispecific antibody.

With the advent of monoclonal antibodies, extensive research has focused on developing cancer therapies that target antigens expressed on the surface of cancer cells[1]. It soon became apparent that, to effectively eradicate tumors, most antibodies needed to be armed or possess an additional function[2]. Several strategies for enhancing antibody-based therapies have shown success, including antibody-drug conjugates (ADCs)[3], Bispecific T-cell Engagers (BiTEs)[4], and related CAR-T cell therapies[5]. However, these approaches demonstrate efficacy in only subsets of patients and are frequently associated with severe side effects. ADCs rely on endocytosis for payload delivery, which limits their ability to effectively deliver cytotoxic agents inside target cells, and their maximum tolerated dose is constrained by the inherent toxicity of the payload[3]. CAR-T and BiTE therapies, while potent, particularly in hematologic malignancies, often trigger severe inflammatory responses[5,6]. In addition, ADCs and CAR-T therapies require complex and expensive manufacturing processes. Consequently, there is an urgent need for new targeted therapies that offer improved efficacy, reduced toxicity, and greater cost efficiency.

As an alternative, another approach has emerged: bispecific apoptosis triggers (BATs), bispecific antibodies designed to target both a tumor-associated antigen and death receptor 5 (DR5 or TNFRSF10B, TRAILR2)[7,8]. Apoptosis induced by DR5 occurs through the extrinsic apoptotic pathway. Upon binding its ligand TRAIL and clustering on the cell surface, DR5 recruits and activates pro-caspase-8 and/or pro-caspase-10. These initiator caspases, once activated, cleave and activate downstream effector caspases, which ultimately leads to apoptotic cell death characterized by DNA fragmentation, membrane blebbing, and cell disassembly[9]. BATs are presumed to selectively accumulate on cancer cells, subsequently engaging and activating DR5 to induce apoptosis and eliminate tumors[7]. However, since effective signaling and apoptosis induction require DR5 clustering, monovalent or bivalent binding to DR5 is insufficient to induce apoptosis[10]. Early BAT development efforts were often based on the premise that binding to an overexpressed tumor-associated antigen would create sufficient molecular crowding to induce DR5 clustering. In this study, we introduce IMV-M, a bispecific antibody targeting the tumor-associated antigens MUC16 and DR5. IMV-M was designed to selectively activate DR5 on MUC16-positive tumors through a unique mechanism that uses the anti-MUC16 antibody component's ability to bind multiple repeats in the MUC16 extracellular domain, bringing multiple IMV-M molecules adjacent to each other and thereby generating DR5 clustering.

Research and Development, ImmuVia Inc, 245 First Street, Suite 1800, Cambridge, MA 02142, USA. ✉email: cso@immuvia.com

Results

The bispecific antibody IMV-M was designed to selectively cluster DR5 on cancer cells

To generate a bispecific antibody that could strongly cluster DR5 on cancer cells, we took advantage of (i) the structure of MUC16, which, unlike the majority of cell surface antigens, contains multiple similar segments (repeats) in its extracellular domain[11], and (ii) Sofituzumab (hu3A5), an anti-MUC16 antibody, which is capable of binding multiple adjacent antibody molecules to the repeats on the same MUC16 molecule[12]. We hypothesized that a bispecific antibody comprised of Sofituzumab fused to an anti-DR5 component could enforce effective DR5 clustering on MUC16-positive cells. To test this hypothesis, we created an antibody with the following structure (Fig. 1a): Sofituzumab IgG antibody was fused with a scFv fragment of a fully human anti-DR5 antibody via a flexible linker to allow an optimal geometry for DR5 clustering and activation. With this design, IMV-M was expected to promote DR5 clustering and subsequent activation on MUC16-positive cells (Fig. 1b), while on MUC16-negative cells, this bispecific antibody could bring together no more than two DR5 molecules (as shown in Fig. 1c). Furthermore, the high affinity of this anti-MUC16 antibody (K_D ~ 0.3–0.9 nM[13]) along with a low-affinity anti-DR5 scFv (K_D ~ 0.2 μM, Supplementary Information), enhanced the selectivity of the construct's interaction with MUC16-positive cancer cells.

IMV-M inhibits proliferation and induces apoptosis of MUC16-positive cells

We evaluated the cytotoxic activity of IMV-M after a two-day exposure in a panel of human MUC16-positive cell lines derived from pancreatic, breast, gastric, ovarian, and non-small cell lung cancers. As selectivity controls, we used the parental anti-MUC16 monospecific antibody and a bispecific antibody, consisting of an anti-fluorescein IgG[14] fused to the same anti-DR5 scFv as used in IMV-M. Exposure of cells to IMV-M (Fig. 2a) resulted in effective cell killing even at the lowest tested concentration (0.16 nM), whereas the anti-MUC16 antibody showed no cytotoxic effect across the entire tested concentration range (0.16–10 nM), and the anti-fluorescein/anti-DR5 bispecific antibody was unable to eradicate the cell populations even at the highest concentration (10 nM). We then evaluated the anti-proliferative and apoptosis-inducing activity of IMV-M in MUC16-positive PK-59 pancreatic adenocarcinoma cell populations in real-time monitoring cell proliferation and apoptosis progression to its final stages in individual cells. Exposure of the cells to IMV-M resulted in a nearly complete arrest of cell proliferation even at the lowest tested concentration (40 pM) within the first 24 h (Fig. 2b) and activation of the effector caspases in most cells within the first 8 h (Fig. 2c). In contrast, the anti-MUC16 antibody showed no effect on cell growth, as cell proliferation remained exponential, and the antibody did not induce apoptosis across the entire range of tested concentrations (40 pM to 10 nM). The anti-fluorescein/anti-DR5 antibody caused only a partial slow-down in cell proliferation and induced apoptosis in a small fraction of PK-59 cells, even at the highest tested concentration (10 nM). These results demonstrate that IMV-M is highly potent and selective in killing MUC16-positive cells via apoptosis.

IMV-M exhibits strong anti-tumor activity in several MUC16-positive xenograft models

To identify xenograft cancer models expressing MUC16, we used immunohistochemistry. NIH:OVCAR-3 xenografts served as a benchmark, as Genentech's ADCs using the same anti-MUC16 antibody were previously tested on NIH:OVCAR-3 xenografts. As shown in Fig. 3 and summarized in Table 1, xenografts derived from various cancer cell lines displayed differing levels of MUC16 expression, ranging from strong (NIH:OVCAR-3) to

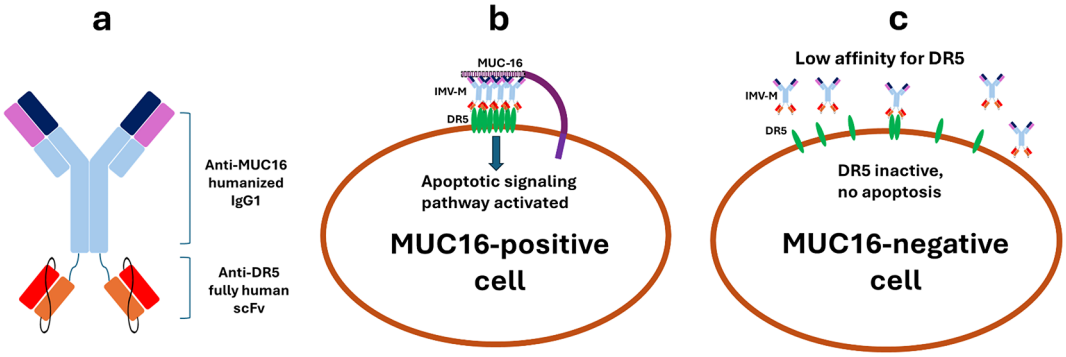

Fig. 1. Design and mode of action of IMV-M. (**a**) IMV-M consists of the high-affinity anti-MUC16 humanized IgG1 antibody hu3A5, fused at its heavy chain C-terminus to a low-affinity scFv fragment of the anti-death receptor 5 (DR5) antibody lexatumumab, connected via a flexible linker. (**b**) Proposed mechanism of action of IMV-M: Multiple IMV-M molecules bind to the repetitive units of the cell surface MUC16 molecule, bringing them into close proximity to each other and the surface DR5 molecules. This proximity promotes the lateral diffusion of multiple DR5 molecules across the membrane, crowding them together. The flexible linker allows the DR5 molecules to align in an optimal geometric configuration, enabling clustering. Once DR5 clustering occurs, extrinsic apoptotic pathway is activated, and the cell undergoes programmed death and elimination. (**c**) IMV-M is designed to exhibit low affinity for DR5 to minimize binding to DR5 on the surface of MUC16-negative cells. Even in the rare instance where the binding occurs, the IMV-M molecules cannot bring together more than two DR5 molecules. These design features ensure that IMV-M cannot induce DR5 clustering or apoptosis in MUC16-negative cells.

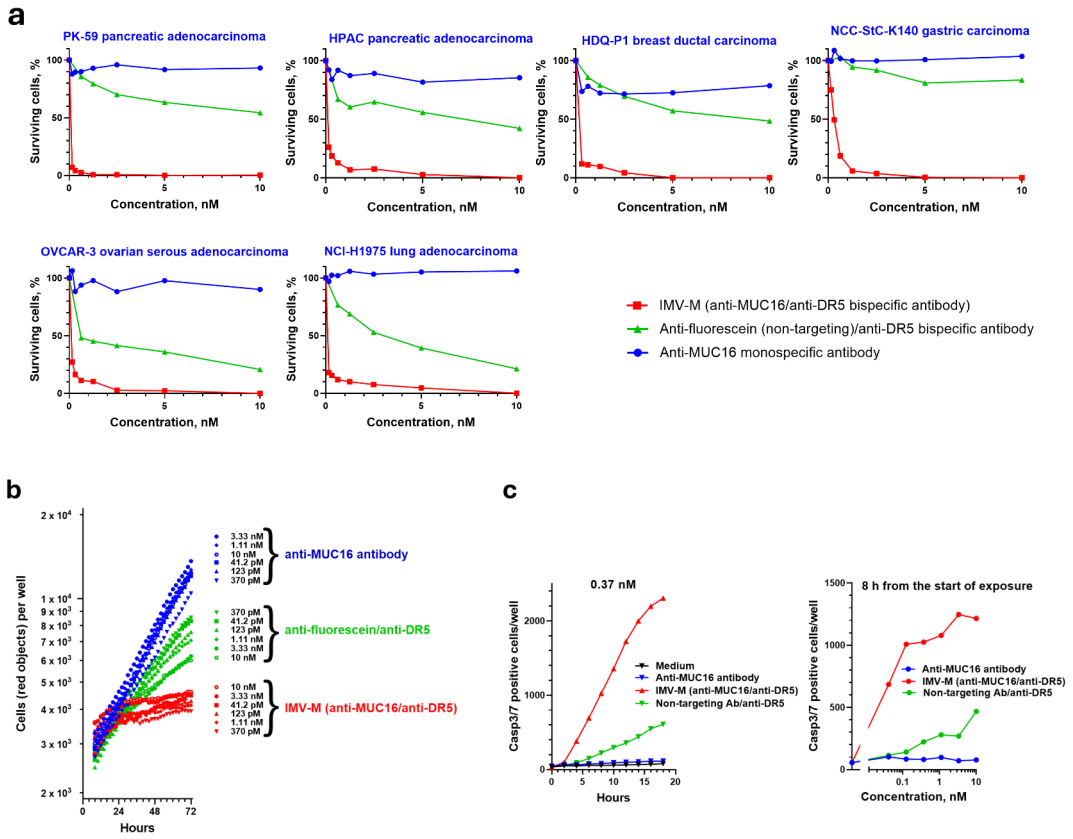

Fig. 2. Cytotoxic effects of IMV-M on MUC16-positive cell lines in vitro. (**a**) IMV-M is selectively cytotoxic to MUC16-positive cell lines derived from pancreatic, breast, gastric, ovarian and non-small cell lung cancers. Cells were treated with various concentrations of IMV-M (red), a bispecific antibody of a similar design incorporating a non-targeting IgG1 and the same anti-DR5 scFv (green), or the monospecific parental anti-MUC16 IgG1 antibody (blue) for 2 days, and the relative number of viable cells was assessed using the CellTiter-Glo assay. (**b**, **c**) IMV-M arrests cell proliferation and induces apoptosis in PK-59 cells. Cells were treated with the same antibody conditions as in (**a**), and individual cell proliferation, (**b**) and apoptosis, (**c**) were monitored in real time using the IncuCyte system as described in Methods. A representative subset of the apoptosis monitoring data is shown in panel c. Similar results were observed across the entire concentration range and throughout all monitored time points.

negative (negligible). Our findings of MUC16 expression closely aligned with data from the Cancer Dependency Map Project at the Broad Institute (https://depmap.org/portal/). We then examined the anti-tumor activity of IMV-M in these xenograft models. In mice bearing established (~130 mm^3) xenografts of the pancreatic adenocarcinoma (PDAC)-derived cell line HPAC, a single intravenous injection of 5 mg/kg IMV-M resulted in pronounced tumor regression, while treatment with either a bispecific antibody containing a non-targeting IgG and the same anti-DR5 component, or with the parental anti-MUC16 monospecific antibody, had no impact on xenograft growth, similar to vehicle control (Fig. 4a). Furthermore, no body weight loss (Supplementary Information) or any gross clinical abnormalities were observed in any animal group during the treatment period, indicating a lack of toxicity from IMV-M in mice. We investigated the dose-dependent anti-tumor activity of IMV-M using a xenograft model derived from the PDAC cell line PK-59. IMV-M demonstrated anti-tumor activity even at the lowest tested single dose of 1 mg/kg, with progressively stronger effects observed at the higher doses of 2.5 mg/kg and 5 mg/kg (Fig. 4b). Similar experiments with treatment at 5 mg/kg were carried out with several other PDAC and non-small cell lung cancer (NSCLC) xenograft models (Fig. 4c-g). IMV-M demonstrated strong anti-tumor activity in three out of five models with moderate MUC16 expression (HPAC, PK-59 and HCC827) and one out of two models with weak MUC16 expression (NCI-H1975). It showed marginal activity in two models with moderate MUC16 expression (Capan-2 and SW1990) and one with low MUC16 expression (NCI-H292).

IMV-M does not affect MUC16-negative xenograft models

To evaluate whether IMV-M may harm MUC16-negative tissues we conducted in vivo studies on xenografts with marginal or no MUC16 expression, based on immunohistochemistry (IHC) results (Fig. 3) and data from the Cancer Dependency Map. IMV-M demonstrated no adverse effects on these xenografts (Fig. 4h-j), reinforcing the likelihood that it would not be toxic to MUC16-negative normal tissues.

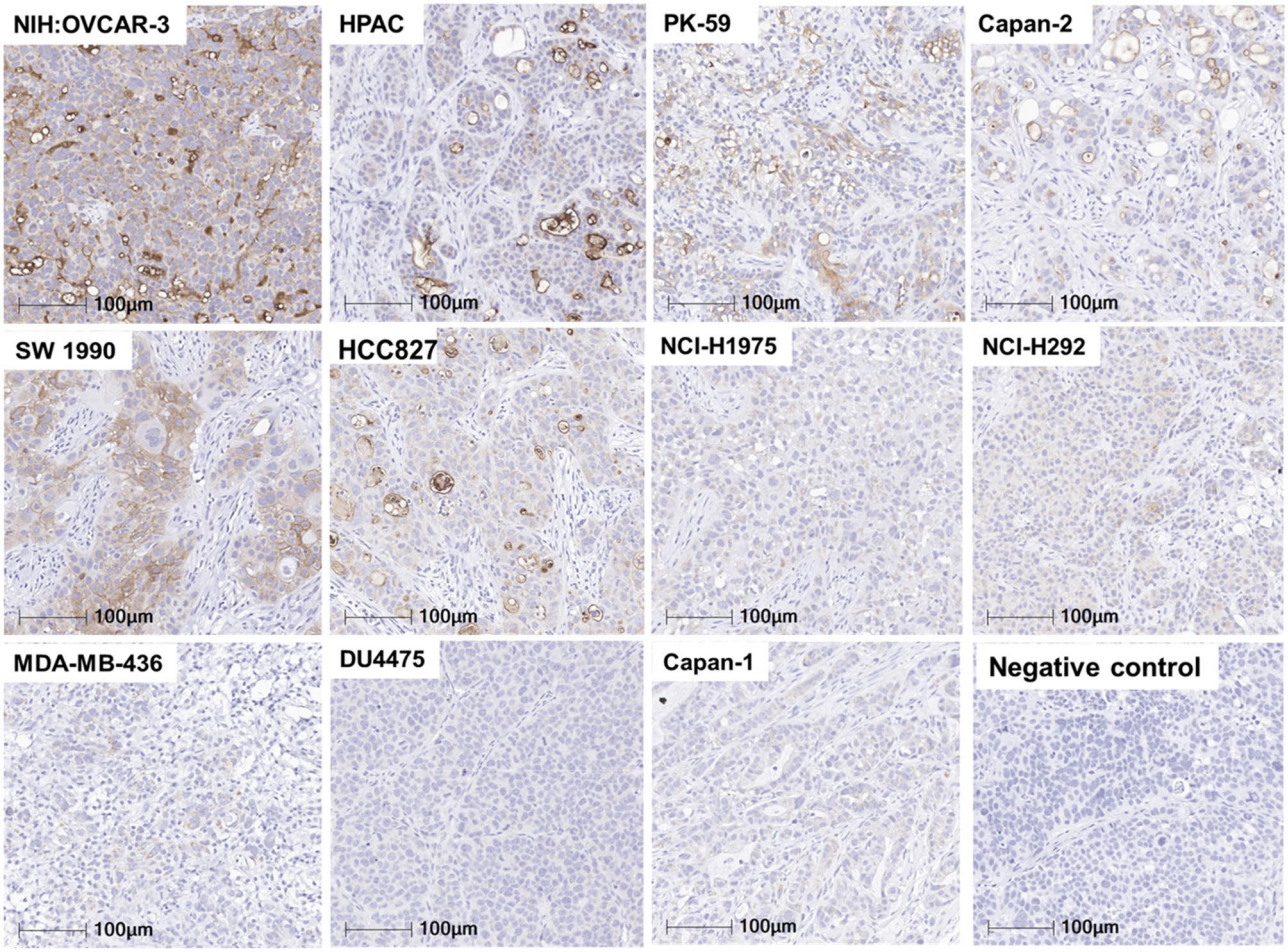

Fig. 3. MUC16 expression in xenografts derived from cancer cell lines. MUC16 protein levels in xenograft tumors generated from cancer cell lines were evaluated using immunohistochemistry with an anti-MUC16 antibody. The summarized results are provided in Table 1.

Cell line	Origin	MUC16 expression
NIH:OVCAR-3	Ovarian adenocarcinoma	Strong
HPAC	PDAC	Moderate
PK-59	PDAC	Moderate
Capan-2	PDAC	Moderate
SW1990	PDAC	Moderate
HCC827	NSCLC	Moderate
NCI-H1975	NSCLC	Weak
NCI-H292	NSCLC	Weak
MDA-MB-436	Breast carcinoma	Negative
DU4475	Breast carcinoma	Negative
Capan-1	PDAC	Negative

Table 1. MUC16 protein levels in tumor xenografts (IHC Fig. 3).

The anti-tumor activity of IMV-M does not require interaction with the Fc gamma receptor II (FcγRIIB)

The in vivo anti-tumor activity of previously reported DR5-targeting monospecific IgG antibodies and the anti-FOLR1/anti-DR5 bispecific antibody depended on secondary crosslinking through interaction with FcγRIIB, which is expressed on B cells present in nude mice[15–17]. In the absence of FcγRIIB interaction, anti-DR5 antibodies lost their anti-tumor activity. This limited capacity of IgG1 anti-DR5 antibodies to cluster DR5 can be attributed to their bivalency, restricting them to linking only two DR5 molecules at a time. To assess whether

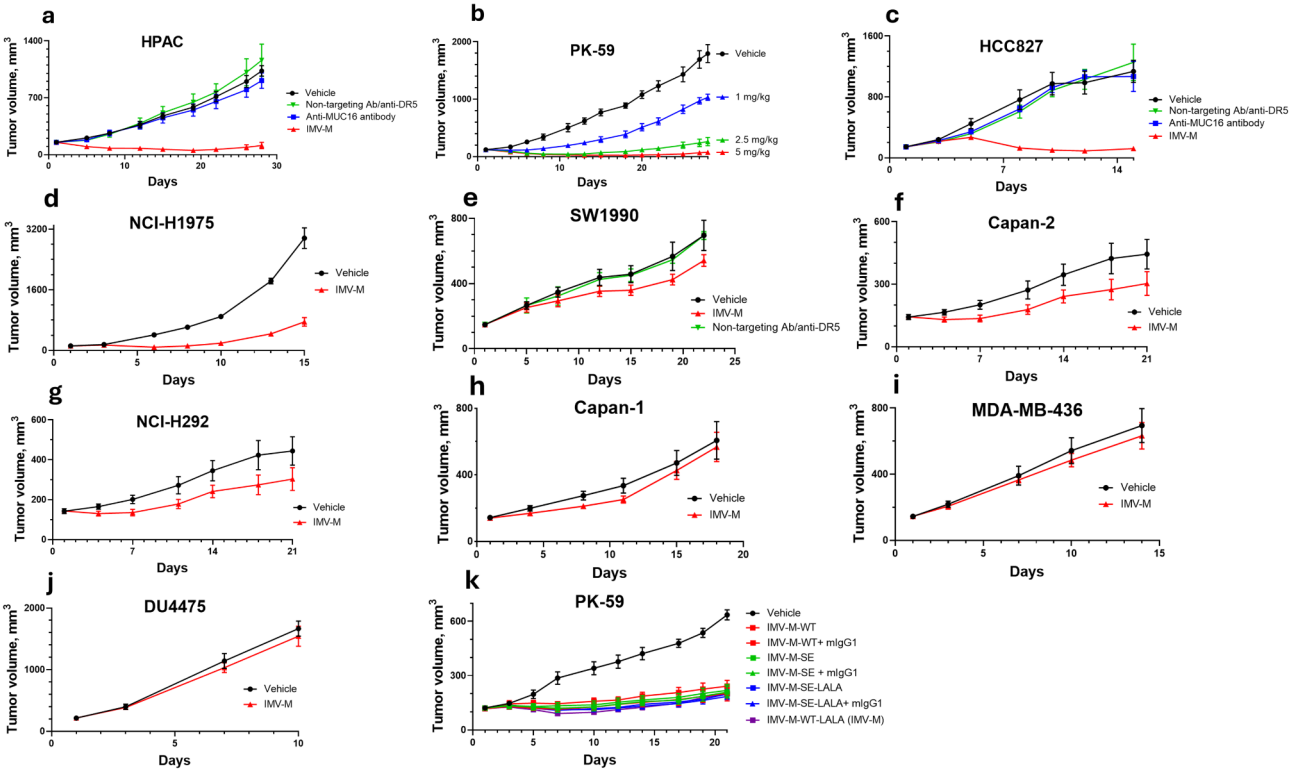

Fig. 4. Anti-tumor activity of IMV-M in vivo in tumor xenograft models. (**a**) Nude mouse bearing established MUC16-positive HPAC PDAC-derived xenografts (~ 130 mm^3) were divided into four cohorts ($n = 5$ mice per group). The cohorts were treated intravenously on day 1 with IMV-M (red), a bispecific antibody of similar design incorporating a non-targeting IgG1 and the same anti-DR5 scFv (green), the monospecific parental anti-MUC16 IgG1 antibody (blue), or vehicle only (black), each at a dose of 5 mg/kg. (**b**) Nude mice bearing established MUC16-positive PK-59 PDAC-derived xenografts (~ 130 mm^3) were treated intravenously on day 1 ($n = 4$ mice per group) with IMV-M (two-step purified) at 1 mg/kg (blue), 2.5 mg/kg (green), 5 mg/kg (red), or vehicle only (black). (**c**–**g**) Additional experiments were conducted using the same design as in a with MUC16-positive xenografts: HCC827 ($n = 5$ mice per group), NCI-H1975 ($n = 5$ mice per group), SW1990 ($n = 5$ mice per group), Capan-2 ($n = 4$ mice per group), and NCI-H292 ($n = 4$ mice per group). (**h**–**j**) Similar experiments were carried out with MUC16-marginal xenografts: Capan-1 ($n = 5$ mice per group), MDA-MB-436 ($n = 4$ mice per group), and DU4475 ($n = 4$ mice per group). (**k**) A separate experiment with MUC16-positive PK-59 xenografts tested variants of IMV-M containing Fc region mutations designed to enhance or reduce its affinity for FcγRIIB ($n = 4$ mice per group). Some groups were co-injected with 30 mg/kg of a non-targeting (anti-fluorescein) mouse IgG1. Data are presented as means ± SEM in all plots.

the anti-tumor activity of IMV-M depended on FcγRIIB interaction, we compared the anti-tumor activities of several IMV-M variants at a 5 mg/kg dose:

1. IMV-M-WT-LALA: Featuring two mutations (L234A and L235A) in the human IgG1 Fc region, which significantly reduce IgG1's affinity for FcγRIIB and other Fcγ receptors[18–21].
2. IMV-M-SE-LALA: Incorporating the L234A and L235A mutations along with an S267E substitution, which selectively restores the affinity of human IgG1 for FcγRIIB[17,22].
3. IMV-M-SE: Containing only the S267E substitution.
4. IMV-M-WT: Featuring no Fc-region mutations.

To simulate the high IgG1 concentration in human patients, which competes with therapeutic antibodies for Fcγ receptor binding, certain groups of mice were co-injected with 30 mg/kg of non-targeting mouse IgG1, achieving an approximate blood concentration of 2 μM. Notably, mouse IgG1 has a higher affinity for mouse FcγRIIB (K_D of 0.3 μM) compared to human IgG1 (K_D of 8 μM)[22,23]. As shown in Fig. 4k, the anti-tumor activity of IMV-M was unaffected by either enhanced or attenuated affinity for FcγRIIB or by the presence or absence of mouse IgG1.

IMV-M exhibits favorable safety and pharmacokinetics in cynomolgus monkeys

Both the anti-MUC16 and anti-DR5 components of IMV-M cross-react with the corresponding cynomolgus monkey antigens (Supplementary Information and [12,24,25]), indicating that the cynomolgus monkey species is a suitable preclinical model for evaluating the systemic toxicity of IMV-M. In a pilot study, two cynomolgus

monkeys were intravenously injected twice with IMV-M, with a 21-day interval between doses; one monkey received 10 mg/kg per dose, and the other received 20 mg/kg per dose. Toxicity was assessed by monitoring hematologic parameters and blood clinical chemistry (Supplementary Information). No abnormalities were observed, indicating an absence of toxicity in this study.

The half-life of IMV-M in the blood of monkeys was also assessed (Supplementary Information). IMV-M circulation half-life was approximately 5–7 days and remained consistent after the second injection. These findings suggest that IMV-M may be sustained in the bloodstream long enough to effectively reach tumors, with no observed immune response leading to its neutralization in monkeys.

Discussion

IMV-M exhibited anti-tumor activity exclusively in xenografts expressing MUC16 and had no effect on MUC16-negative xenograft models, which were used to mimic healthy tissues. This demonstrates that MUC16 expression is a prerequisite for its anti-tumor activity. IMV-M had pronounced anti-tumor activity with three out of five xenografts with moderate MUC16 expression, and one out of two xenografts with weak MUC16 expression showing the tendency that a higher MUC16 expression was a favorable factor for a stronger activity. There was variability in the response of xenograft models to IMV-M. In two xenografts with moderate MUC16 expression and one with weak expression, IMV-M demonstrated only marginal anti-tumor activity. While further studies are needed to better understand this phenomenon, prior observations with ADCs provide some insights. Several key factors may contribute to the variability in xenograft response to IMV-M, despite comparable antigen expression. As shown in previous ADC studies, variations in vascular permeability and interstitial transport can lead to heterogeneous ADC distribution, affecting therapeutic outcomes[26]. Additionally, the ability of an ADC to induce bystander killing of neighboring antigen-negative cells may vary across tumor models[27]. While the bystander effect was reported in several bispecific antibodies targeting DR5[7], we have not evaluated the ability of IMV-M to induce bystander cytotoxicity. A study evaluating PSMA-ADC efficacy in patient-derived prostate cancer xenografts found significant variability in treatment response despite comparable PSMA expression levels[28]. This suggests that factors beyond antigen expression, such as the tumor microenvironment and intrinsic cellular properties, play a critical role in ADC efficacy. Even within the same tumor model, subpopulations of cells with different antigen levels can result in mixed treatment responses[28]. These examples highlight the need for a comprehensive evaluation of tumor characteristics beyond antigen expression to optimize therapeutic strategies for IMV-M.

DR5 is an attractive target for inducing apoptosis in tumor cells, as it is broadly expressed across various cancers at levels sufficient to trigger apoptosis upon clustering and is upregulated in tumors relative to normal tissues[7]. Directly assessing the degree of DR5 clustering remains challenging[10], making it unfeasible to compare anti-DR5 agents based on their clustering efficiency. However, preclinical in vivo antitumor activity serves as a valuable indirect indicator. Among previously reported agents, the anti-FOLR1/anti-DR5 bispecific antibody BaCa[17] exhibited no anti-tumor activity in xenograft models in mice unless the S267E mutation was introduced into the Fc region of IgG1. This mutation enabled BaCa to engage Fcγ receptor IIB on B cells, providing secondary cross-linking[15,16]. Nude mice used for xenograft experiments have B cells, which can infiltrate tumors, but these mice have low levels IgG1 antibodies in their blood[29,30], while concentration of IgG1 in human blood is very high and likely impeding the interaction of therapeutic antibodies with Fcγ receptor IIB in humans. As shown in Fig. 4k, the anti-tumor activity of IMV-M was robust and unaffected by either enhanced or attenuated affinity for FcγRIIB or by the presence or absence of mouse IgG1. ENb-TRAIL, an EGFR-targeted nanobody fused to a TRAIL derivative[31] binds both death receptor 4 and death receptor 5, forming a trivalent interaction on both sides with potential super-clustering of death receptors. ENb-TRAIL exhibited cytotoxic and apoptosis-inducing activity in vitro and demonstrated anti-tumor efficacy in vivo using an unconventional delivery method. The delivered dose and versatility of ENb-TRAIL's in vivo activity remain unclear. RG7386[32], a bispecific tetravalent antibody targeting FAP, an antigen expressed on tumor stromal cells and some cancer cells, and DR5, induced apoptosis in FAP-positive tumor cell lines and in mixed populations of tumor cells and FAP-expressing cells. RG7386 generally required high, multiple doses and/or combination with chemotherapy for efficacy. Its limited effectiveness in vivo may have been due to the spatial distribution of tumor cells in patient tumors, where not all cancer cells were in proximity to FAP-expressing stromal cells. In a clinical trial, RG7386 demonstrated marginal clinical activity[33], leading to the discontinuation of its clinical development. A mixture of two self-oligomerizing anti-DR5 antibodies, HexaBody-DR5/DR5[34,35] was designed to induce DR5 super-clustering. In preclinical studies, HexaBody-DR5/DR5 often required multiple doses for even a moderate activity in solid tumor models, except in the highly DR5-sensitive COLO-205 model[34]; its activity in multiple myeloma was dependent on chemotherapy[35]. During a clinical trial, many patients experienced serious adverse events, likely, due to an indiscriminate targeting of DR5. Due to these safety concerns and insufficient antitumor activity (https://www.hra.nhs.uk/planning-and-improving-research/application-summaries/research-summaries/gen1029-in-patients-with-malignant-solid-tumours/?utm_source=chatgpt.com), the study was terminated, and clinical development of HexaBody-DR5/DR5 was discontinued. García-Martínez and colleagues reported two bispecific antibodies targeting DR5: one directed against cadherin 17 (BI 905711)[24] and, more recently, another targeting cadherin 3[36]. In preclinical studies, BI 905711 demonstrated anti-tumor activity in several xenograft models; however, the interpretation of its efficacy was challenging due to the inconsistent tumor growth in these models. In a Phase 1 trial[37], BI 905711 exhibited only modest clinical activity, leading to the discontinuation of its clinical development. The bispecific antibody targeting cadherin 3 and DR5 demonstrated promising in vivo activity[36]. Interestingly, cadherin 3 has five extracellular domain repeats, though it remains undisclosed whether the antibody binds to these repeats. Among other DR5-targeting agents that entered clinical trials were two TRAIL derivatives, Aponermin[38] and Eftozanermin α[39] and two multivalent anti-DR5 antibodies, Aplitabart[40] and Ozekibart[41]. Of these, Eftozanermin α exhibited only moderate preclinical activity, even with multiple doses,

or in combination with chemotherapy[39]. In Phase 1 trials (NCT03082209 and NCT04570631), Eftozanermin α had modest clinical activity and its development was discontinued. In a preclinical study, Aplitabart[40] required multiple high doses and showed only modest efficacy without additional chemotherapy. The clinical efficacy data for Aplitabart have not been publicly disclosed; its development was apparently stopped. Aponermin and Ozekibart, have shown promising results, and ongoing research continues to explore their potential as cancer therapies. Aponermin was approved in China for use in combination with thalidomide and dexamethasone for the treatment of patients with relapsed or refractory multiple myeloma[42]. Ozekibart, when combined with established chemotherapy regimens, shows promise as a potential treatment for advanced colorectal cancer (Inhibrx Biosciences January 2025 announcement). Thus, many anti-death receptor agents, had achieved only limited success in both preclinical and clinical studies. Agents with minimal preclinical activity demonstrated negligible clinical efficacy, while those showing moderate preclinical effects similarly yielded only modest outcomes in clinical trials or were too toxic. IMV-M was designed with an additional DR5 clustering mechanism distinct from those of other DR5-targeting agents, with one possible exception (anti-cadherin 3/anti-DR5)—by clustering multiple IMV-M molecules on a single antigen molecule. IMV-M exhibits robust anti-tumor activity across diverse xenograft models.

MUC16 is a promising therapeutic target, as it is overexpressed in the tumors of most ovarian cancer patients and in a significant proportion of patients with pancreatic adenocarcinoma (PDAC) and non-small cell lung cancer (NSCLC). It is also present in subsets of patients with other cancers, including endometrial, breast, esophageal, gastric, and colorectal adenocarcinomas[43–55]. MUC16 is largely absent in most normal tissues, appearing only on the free surface of select epithelia[56,57] [http://gepia.cancer-pku.cn; www.humanproteomemap.org; www.proteinatlas.org], which minimizes its exposure to circulating IMV-M.

Additional evidence supporting IMV-M's clinical promise comes from studies with two ADCs developed by Genentech, DMUC5754A and DMU46064A, which utilize the same anti-MUC16 antibody, hu3A5. Preclinical evaluations of these conjugates showed activity primarily in xenograft models with very high MUC16 expression, such as NIH:OVCAR-3 or greater[12,13], and only at doses close to or exceeding their maximal tolerated doses in patients. Despite limited preclinical efficacy, these ADCs—especially DMU46064A—demonstrated promising activity (but narrow therapeutic window due to payload-related toxicity) in early clinical trials[58,59]. Given IMV-M's robust efficacy in xenograft models with MUC16 expression levels notably lower than NIH:OVCAR-3 (Fig. 3) at doses several-fold lower than the predicted tolerable dose, it is likely to exhibit favorable clinical activity.

MUC16 undergoes proteolytic cleavage, leading to the shedding of its extracellular domain into the bloodstream. This process is essential for the release of the cleaved MUC16 fragment, known as CA125, which serves as a biomarker for ovarian cancer[60]. A key question is whether circulating shed MUC16 could hinder tumor targeting with IMV-M. The results from Phase 1 clinical studies of two ADCs utilizing the same anti-MUC16 antibody provide valuable insights. Despite MUC16 being a poorly internalizing antigen—significantly limiting the anti-tumor efficacy of these ADCs (both were active only in preclinical models with exceedingly high MUC16 expression[12,13])—there were clear indicators of clinical activity[58,59]. These included objective tumor responses at doses as low as 0.8 mg/kg and a sharp decline in CA125 levels in most patients by day 21 of treatment. These findings are encouraging, suggesting that a dose as low as 0.8 mg/kg is not neutralized by circulating MUC16.

IMV-M offers an effective and safe alternative to MUC16-targeting ADCs: (i) IMV-M acts directly on the cell surface, while ADCs require internalization and lysosomal degradation to activate. Given MUC16's low internalization efficiency, ADCs need very high MUC16 expression levels to be effective, whereas IMV-M demonstrated activity in xenografts with moderate MUC16 expression. (ii) IMV-M's cell-killing mechanism is independent of drug resistance often acquired in chemotherapy-pretreated patients, making its activity less likely to be impacted by such resistance. (iii) The maximum tolerated dose of ADCs is limited by the inherent toxicity of their payload, leading to a narrow therapeutic window, as seen with DMUC5754A and DMU46064A. Other types of MUC16-targeting therapies have shown limited success to date. Clinical trials of a MUC16-targeted CAR-T and a BiTE (Ubamatamab) have reported disappointing results[61,62]. There is evidence suggesting that IMV-M will be safe for patients: (i) no signs of toxicity were observed in cynomolgus monkeys; (ii) the DR5 component in IMV-M is a fragment of the antibody Lexatumumab, which was well tolerated by patients in clinical trials[63–65]; (iii) no MUC16-related toxicity was observed in clinical trials of the two MUC16-targeted ADCs, and the systemic toxicity observed was consistent with the typical profile of ADCs using this cytotoxic payload[58,59].

Methods

Cell culture

HPAC (CRL-2119), NIH:OVCAR-3 (HTB-161), NCI-H1975, SW1990, NCI-H292, Capan-1, Capan-2, DU4475, MDA-MB-436, NCI-H1975, and HCC827 were obtained from the American Type Culture Collection (ATCC). PK-59 was obtained from Cobioer Biosciences Co., Ltd and the RIKEN BioResource Research Center. NCC-StC-K140 was obtained from RIKEN, and HDQ-P1 was obtained from The Leibniz Institute DSMZ – German Collection of Microorganisms and Cell Cultures GmbH.

Expression of IMV-M and control proteins

Monospecific and bispecific antibodies for this study were generated at WuXi Biologics and BioIntron using standard transient expression procedures in CHO cells, followed by isolation through protein A chromatography. When indicated, additional purification was performed using MSS-Superdex 200 chromatography. The integrity and purity of the antibodies were assessed using reduced and non-reduced SDS-PAGE and SEC-HPLC.

In vitro cytotoxicity and apoptosis testing

The CellTiter-Glo tests (Promega Corporation) were performed at Pharmaron and HD Biosciences (WuXi AppTec). Cells were plated into flat-bottom tissue culture 96-well plates. The following day, test reagents were added for an additional two days. The relative number of viable cells was then assessed using the CellTiter-Glo assay, following the standard manufacturer's protocol. Inhibition of cell proliferation and activation of apoptosis in PK-59 cells were examined by monitoring individual cells in real time using the Incucyte S3, a live-cell imaging and analysis system (Sartorius AG) at Pharmaron. Cells were plated into a 96-well flat tissue culture plate at a density of 1500 cells/well. The following day, test reagents and monitoring dyes were added to the cells, and fluorescent images of individual cells were captured every two hours following the manufacturer's protocol. Incucyte Nuclight Rapid Red Dye for nuclear labeling (Sartorius Cat. No. 4717) and Incucyte® Caspase-3/7 Green Dye for Apoptosis (Sartorius Cat. No. 4440) were used to detect cell proliferation (number of red-fluorescent objects) and apoptosis (number of green-fluorescent objects with activated caspase-3 and/or 7) to monitor the execution phase of apoptosis. All conditions in the in vitro cytotoxicity and apoptosis assays were tested in triplicate, and the mean values of a representative experiment were plotted. The SEM values were very small and therefore most would not be visible on the plots.

Immunohistochemistry (IHC) study

This study was performed at HD Biosciences (WuXi AppTec). Tumor tissues embedded in paraffin were cut with a microtome to a thickness of 4 µm. After heat-induced antigen retrieval in Citrate 6.0 (MXB #MVS0066), sections were immersed in a 3% hydrogen peroxide solution for 5 min. To avoid nonspecific staining, sections were then incubated in Dako REAL™ Antibody Diluent (Code S2022) supplemented with 5% normal goat serum (Kangyuan #KY-01021) for 30 min at room temperature, followed by exposure to the anti-MUC16 antibody (Abcam #110640) at a 1:500 dilution in the same buffer overnight. The sections were then treated with HRP-conjugated Polyclonal Goat anti-Rabbit Immunoglobulins (Dako, cat# 4003) and visualized with diaminobenzidine according to the manufacturer's protocol. The nuclei were stained with hematoxylin. Slides were scanned using an Aperio Scanner: Versa 8 (Leica) at 200X magnification. Images were opened with HALO software, and the pen tool was used to create an annotation layer, with necrotic areas excluded from the annotation layer.

Mouse xenograft studies

These studies were conducted at Pharmaron and HD Biosciences (WuXi AppTec). All procedures related to animal handling, care, and treatment were performed according to guidelines approved by the Institutional Animal Care and Use Committee (IACUC) of HD Biosciences, adhering to the standards set by the Association for Assessment and Accreditation of Laboratory Animal Care (AAALAC). BALB/c nude female mice (GemPharmatech Co., Ltd., Beijing, China), aged 6–8 weeks at the time of inoculation and weighing 16–20 g, were used for the study. Tumor cells in the exponential growth phase were used for inoculation. Each mouse was inoculated subcutaneously on the right flank with tumor cells to establish tumor growth. Treatments were initiated when the mean tumor volume reached approximately 130 mm^3. Mice were randomly assigned to treatment groups based on tumor volume to ensure similar average starting tumor sizes across groups. The test compounds were administered intravenously via the tail vein. Throughout the study, mice were monitored for tumor growth and general health, including behavior, mobility, food and water consumption, body weight, eye/hair condition, and other signs of abnormal effects. The studies are reported in accordance with ARRIVE guidelines. The measurement of tumor size was conducted twice weekly with a caliper and the tumor volume (mm^3) is estimated using the formula: TV = a × b × b/2, where "a" and "b" are long and short diameters of a tumor, respectively. The TVs are used for calculation of the tumor growth inhibition and tumor growth delay. For the tumor growth inhibition (TGI), the value using the formula:

$$\text{a. } \%\ \Delta T/\Delta C = (\text{TreatedTVfinal} - \text{TreatedTVinitial})/(\text{VehicleTVfinal} - \text{VehicleTVinitial}) \times 100.$$

$$\text{b. } \%\ \text{TGI} = (1 - \Delta T/\Delta C) \times 100.$$

The "TVfinal" and "TVinitial" are the mean tumor volumes on the final day and initial day of dosing.

Statistical tests were conducted, and the level of significance was set at 5% or $P < 0.05$. The group means, standard deviations were calculated for all measurement parameters as study designed. Chi-square test and Two-way RM ANOVA followed by Tukey's correction for multiple comparisons were applied among groups. Statistical difference between the positive and control groups in Fig. 4a-d, k were highly significant with $P < 0.01$–0.001, except Fig. 4b 1 mg/kg ($P < 0.05$). Statistical difference between the positive and control groups in Fig. 3e-j had $P > 0.05$.

Exploratory non-GLP toxicokinetics and safety assessment in non-human primates

Two naïve female cynomolgus monkeys (WuXi AppTec Co., Ltd., Nanjing, Jiangsu Province, 210031, China) were used in this study. All procedures related to animal handling, care, and treatment were performed according to guidelines approved by the Institutional Animal Care and Use Committee (IACUC) of WuXi AppTec, adhering to the standards set by the Association for Assessment and Accreditation of Laboratory Animal Care (AAALAC). Animal 1 received IMV-M (IMV-M-WT-LALA with a two-step purification) via intravenous bolus administration at a dose of 10 mg/kg on Days 1 and 22, while Animal 2 received IMV-M via intravenous bolus administration at 20 mg/kg on the same days. Serum samples were collected at various time points, and IMV-M concentrations were measured using an enzyme-linked immunosorbent assay (ELISA), as described in Supplementary Information. Hematology and clinical chemistry samples were collected at multiple time points.

Hematology parameters analyzed included leukocyte count, red blood cell (RBC) distribution width, erythrocyte count, platelet count, hemoglobin, mean platelet volume, hematocrit, white blood cell (WBC) differential, mean corpuscular volume, mean corpuscular hemoglobin, reticulocyte count, and mean corpuscular hemoglobin concentration. Clinical chemistry parameters analyzed included alanine aminotransferase, creatinine, aspartate aminotransferase, calcium, total protein, phosphorus, albumin, total cholesterol, globulin, triglycerides, albumin/globulin ratio, total bilirubin, alkaline phosphatase, sodium, γ-glutamyltransferase, potassium, glucose, chloride, urea, and creatine kinase. The study is reported in accordance with ARRIVE guidelines.

Data availability

Derived data supporting the findings of this study and all amino acid sequences are available from the corresponding author upon request.

Received: 21 January 2025; Accepted: 10 March 2025
Published online: 22 March 2025

References

1. Farah, R. A., Clinchy, B., Herrera, L. & Vitetta, E. S. The development of monoclonal antibodies for the therapy of cancer. *Crit. Rev. Eukar Gene Expr*. **8**, 321–356 (1998).
2. Delgado, M. & Garcia-Sanz, J. A. Therapeutic monoclonal antibodies against cancer: present and future. *Cells* **12**, 2837 (2023).
3. Khongorzul, P., Ling, C. J., Khan, F. U., Ihsan, A. U. & Zhang, J. Antibody–drug conjugates: a comprehensive review. *Mol. Cancer Res.* **18**, 3–19 (2020).
4. Fenis, A., Demaria, O., Gauthier, L., Vivier, E. & Narni-Mancinelli, E. New immune cell engagers for cancer immunotherapy. *Nat. Rev. Immunol.* **24**, 471–486 (2024).
5. Gajra, A. et al. Barriers to chimeric antigen receptor T-Cell (CAR-T) therapies in clinical practice. *Pharm. Med.* **36**, 163–171 (2022).
6. Khushboo, B. & Kumar, J. R. Perils and problems in bispecific T-Cell engager antibodies. *Curr. Drug Saf.* https://doi.org/10.2174/0115748863286774240219094217 (2024).
7. Goldmacher, V. S., Gershteyn, I. M. & Kovtun, Y. Beyond ADCs: Harnessing bispecific antibodies to directly induce apoptosis for targeted tumor eradication. *Antib. Therapeut*. **7**, 361–360 (2024).
8. Klein, C. et al. The present and future of bispecific antibodies for cancer therapy. *Nat. Rev. Drug Discov*. **23**, 301–319 (2024).
9. Ashkenazi, A. & Dixit, V. M. Apoptosis control by death and decoy receptors. *Curr. Opin. Cell. Biol.* **11**, 255–260 (1999).
10. Valley, C. C. et al. Tumor necrosis factor-related apoptosis-inducing ligand (TRAIL) induces death receptor 5 networks that are highly organized. *J. Biol. Chem.* **287**, 21265–21278 (2012).
11. Das, S. & Batra, S. K. Understanding the unique attributes of MUC16 (CA125): potential implications in targeted therapy. *Cancer Res.* **75**, 4669–4674 (2015).
12. Chen, Y. et al. Armed antibodies targeting the mucin repeats of the ovarian cancer antigen, MUC16, are highly efficacious in animal tumor models. *Cancer Res.* **67**, 4924–4932 (2007).
13. Junutula, J. R. et al. Site-specific conjugation of a cytotoxic drug to an antibody improves the therapeutic index. *Nat. Biotechnol.* **26**, 925–932 (2008).
14. Jung, S., Honegger, A. & Plückthun, A. Selection for improved protein stability by phage display. *J. Mol. Biol.* **294**, 163–180 (1999).
15. Li, F. & Ravetch, J. V. Antitumor activities of agonistic anti-TNFR antibodies require differential FcγRIIB coengagement in vivo. Proc. Natl. Acad. Sci. U.S.A. 110, 19501–19506 (2013).
16. Bournazos, S., Wang, T. T. & Ravetch, J. V. The role and function of Fcγ receptors on myeloid cells. *Microbiol. Spectr.* **4**, (2016). 4.6.20.
17. Shivange, G. et al. A Single-Agent Dual-Specificity targeting of FOLR1 and DR5 as an effective strategy for ovarian cancer. *Cancer Cell.* **34**, 331–345 (2018).
18. Wilkinson, I. et al. Fc-engineered antibodies with immune effector functions completely abolished. *PLoS ONE*. **16**, e0260954 (2021).
19. Hessell, A. J. et al. Fc receptor but not complement binding is important in antibody protection against HIV. *Nature* **449**, 101–104 (2007).
20. Xu, D. et al. In vitro characterization of five humanized OKT3 effector function variant antibodies. *Cell. Immunol.* **200**, 16–26 (2000).
21. Leabman, M. K. et al. Effects of altered FcγR binding on antibody pharmacokinetics in cynomolgus monkeys. *mAbs* **5**, 896–903 (2013).
22. Li, F. & Ravetch, J. V. Apoptotic and antitumor activity of death receptor antibodies require inhibitory Fcγ receptor engagement. Proc. Natl. Acad. Sci. U.S.A. 109, 10966–10971 (2012).
23. White, A. L. et al. Interaction with FcγRIIB is critical for the agonistic activity of anti-CD40 monoclonal antibody. *J. Immunol.* **187**, 1754–1763 (2011).
24. Garcia-Martinez, J. M. et al. Selective tumor cell apoptosis and tumor regression in CDH17-positive colorectal cancer models using BI 905711, a novel liver-sparing TRAILR2 agonist. *Mol. Cancer Ther.* **20**, 96–108 (2021).
25. US Patent 7723485.
26. Bussing, D. et al. Pharmacokinetics of monoclonal antibody and antibody fragments in the mouse eye following systemic administration. *AAPS J.* **23**, 116 (2021).
27. Li, F. et al. Intracellular released payload influences potency and bystander-killing effects of antibody-drug conjugates in preclinical models. *Cancer Res*. **76**, 2710–2719 (2016).
28. DiPippo, V. A. et al. Efficacy studies of an antibody-drug conjugate PSMA-ADC in patient-derived prostate cancer xenografts. *Prostate* **75**, 303–313 (2015).
29. Bloemmen, J. & Eyssen, H. Immunoglobulin levels of sera of genetically thymusless (nude) mice. *Eur. J. Immunol.* **3**, 117–118 (1973).
30. Mink, J. G. et al. Serum immunoglobulins in nude mice and their heterozygous littermates during ageing. *Immunology* **40**, 539–545 (1980).
31. Zhu, Y. et al. Bi-specific molecule against EGFR and death receptors simultaneously targets proliferation and death pathways in tumors. *Sci. Rep.* **7**, 2602 (2017).
32. Brunker, P. et al. RG7386, a novel tetravalent FAP-DR5 antibody, effectively triggers FAP-dependent, avidity-driven DR5 hyperclustering and tumor cell apoptosis. *Mol. Cancer Ther.* **15**, 946–957 (2016).
33. Bendell, J. et al. Phase 1 trial of RO6874813, a novel bispecific FAP-DR5 antibody, in patients with solid tumors. *Mol. Cancer Ther.* **17** (1 Suppl), AbstractA092 (2018).

34. Overdijk, M. B. et al. Dual epitope targeting and enhanced hexamerization by DR5 antibodies as a novel approach to induce potent antitumor activity through DR5 agonism. *Mol. Cancer Ther.* **19**, 2126–2138 (2020).
35. van der Horst, H. J. et al. Potent preclinical activity of HexaBody-DR5/DR5 in relapsed and/or refractory multiple myeloma. *Blood Adv.* **5**, 2165–2172 (2021).
36. Jung, P. et al. A TRAILR2/CDH3 bispecific antibody demonstrates selective apoptosis and tumor regression in CDH3-positive pancreatic cancer. *MABS* **16**, 2438173 (2024).
37. Kopetz, S. et al. A phase Ia/Ib, open-label, dose escalation study of the TRAILR2 agonist BI 905711 in combination with chemotherapy (CT) in patients (pts) with advanced GI cancers. *J. Clin. Oncol.* **41**, 4_suppl TPS820, 820 (2023).
38. Xia, Z. et al. Aponermin or placebo in combination with thalidomide and dexamethasone in the treatment of relapsed or refractory multiple myeloma (CPT-MM301): a randomised, double-blinded, placebo-controlled, phase 3 trial. *BMC Cancer*. **23**, 980 (2023).
39. Phillips, D. C. et al. Hexavalent TRAIL fusion protein eftozanermin alfa optimally clusters apoptosis-inducing TRAIL receptors to induce on-target antitumor activity in solid tumors. *Cancer Res.* **81**, 3402–3414 (2021).
40. Wang, B. T. et al. Multimeric anti-DR5 IgM agonist antibody IGM-8444 is a potent inducer of cancer cell apoptosis and synergizes with chemotherapy and BCL-2 inhibitor ABT-199. *Mol. Cancer Ther.* **20**, 2483–2494 (2021).
41. Subbiah, V. et al. Preclinical characterization and phase I trial results of INBRX-109, a third-generation, recombinant, humanized, death receptor 5 agonist antibody, in chondrosarcoma. *Clin. Cancer Res.* **29**, 2988–3003 (2023).
42. Dhillon, S. Aponermin: first approval. *Drugs* **84**, 459–466 (2024).
43. Chauhan, S. C. et al. Aberrant expression of MUC4 in ovarian carcinoma: diagnostic significance alone and in combination with MUC1 and MUC16 (CA125). *Mod. Pathol.* **19**, 1386–1394 (2006).
44. Iwamoto, M., Nakatani, Y., Fugo, K., Kishimoto, T. & Kiyokawa, T. Napsin A is frequently expressed in clear cell carcinoma of the ovary and endometrium. *Hum. Pathol.* **46**, 957–962 (2015).
45. Rosen, D. G. et al. Potential markers that complement expression of CA125 in epithelial ovarian cancer. *Gynecol. Oncol.* **99**, 267–277 (2005).
46. Kakimoto, S. et al. Significance of mesothelin and CA125 expression in endometrial carcinoma: a retrospective analysis. *Diagn. Pathol.* **16**, 28 (2021).
47. Lakshmanan, I. et al. MUC16 regulates TSPYL5 for lung cancer cell growth and chemoresistance by suppressing p53. Clin. *Cancer Res.* **23**, 3906–3917 (2017).
48. Tu, J. et al. Expression of mucin family proteins in non-small-cell lung cancer and its role in evaluation of prognosis. *J. Oncol.* **2022**, 4181658 (2022).
49. Kanwal, M., Ding, X. J., Song, X., Zhou, G. B. & Cao, Y. MUC16 overexpression induced by gene mutations promotes lung cancer cell growth and invasion. *Oncotarget* **9**, 12226–12239 (2018).
50. Jiang, K. et al. Cancer antigen 125 (CA125, MUC16) protein expression in the diagnosis and progression of pancreatic ductal adenocarcinoma. *Appl. Immunohistochem. Mol. Morphol.* **25**, 620–623 (2017).
51. Haridas, D. et al. Pathobiological implications of MUC16 expression in pancreatic cancer. *PLoS ONE*. **6**, e26839 (2011).
52. Jonckheere, N. & Van Seuningen, I. Integrative analysis of the cancer genome atlas and cancer cell lines encyclopedia large-scale genomic databases: MUC4/MUC16/MUC20 signature is associated with poor survival in human carcinomas. *J. Transl Med.* **16**, 259 (2018).
53. Macdonald, F., Downing, R. & Allum, W. Expression of CA125 in pancreatic carcinoma and chronic pancreatitis. *Br. J. Cancer*. **58**, 505–506 (1988).
54. Streppel, M. M. et al. Mucin 16 (cancer antigen 125) expression in human tissues and cell lines and correlation with clinical outcome in adenocarcinomas of the pancreas, esophagus, stomach, and colon. *Hum. Pathol.* **43**, 1755–1763 (2012).
55. Einama, T. Co-expression of mesothelin and CA125 correlates with unfavorable patient outcome in pancreatic ductal adenocarcinoma. *Pancreas* **40**, 1276–1282 (2011).
56. Davies, J. R., Kirkham, S., Svitacheva, N., Thornton, D. J. & Carlstedt, I. MUC16 is produced in tracheal surface epithelium and submucosal glands and is present in secretions from normal human airway and cultured bronchial epithelial cells. *Int. J. Biochem. Cell. Biol.* **39**, 1943–1954 (2007).
57. Dharmaraj, N. et al. Expression of the transmembrane mucins, MUC1, MUC4 and MUC16, in normal endometrium and in endometriosis. *Hum. Reprod.* **29**, 1730–1738 (2014).
58. Liu, J. F. et al. Phase I study of safety and pharmacokinetics of the anti-MUC16 antibody–drug conjugate DMUC5754A in patients with platinum-resistant ovarian cancer or unresectable pancreatic cancer. *Ann. Oncol.* **27**, 2124–2130 (2016).
59. Liu, J. et al. An open-label phase I dose-escalation study of the safety and pharmacokinetics of DMUC4064A in patients with platinum-resistant ovarian cancer. *Gynecol. Oncol.* **163**, 473–480 (2021).
60. Haridas, D. et al. MUC16: molecular analysis and its functional implications in benign and malignant conditions. *FASEB J.* **28**, 4183–4199 (2014).
61. Moore, K. N. et al. 41P phase I analysis of Ubamatamab (MUC16xCD3 bispecific antibody) in patients with recurrent ovarian cancer. *ESMO Open.* **8**, Suppl. 1, 100821 (2023).
62. O'Cearbhaill, R. E. et al. A phase I clinical trial of autologous chimeric antigen receptor (CAR) T cells genetically engineered to secrete IL-12 and to target the MUC16ecto antigen in patients (pts) with MUC16ecto+ recurrent high-grade serous ovarian cancer (HGSOC). *Gynecol. Onc*. **159**, Suppl. 1, 42 (2020).
63. Plummer, R. et al. Phase 1 and Pharmacokinetic study of lexatumumab in patients with advanced cancers. *Clin. Cancer Res.* **13**, 6187–6194 (2007).
64. Wakelee, H. A. et al. Phase I and pharmacokinetic study of lexatumumab (HGS-ETR2) given every 2 weeks in patients with advanced solid tumors. *Ann. Oncol.* **21**, 376–381 (2009).
65. Harding, J. J. et al. A phase Ia/b first-in-human, open-label, multicenter study of BI 905711, a bispecific TRAILR2 agonist, in patients with advanced gastrointestinal cancers. *J. Clin. Oncol.* **41**, No. 4 Suppl. 115 (2023).

Acknowledgements

This work was supported by ImmuVia Inc.

Author contributions

V.S.G., I.G., R.C. and Y.K. V.S.G. conceived and designed the study and analyzed the data. All authors contributed to the writing of the manuscript.

Declarations

Competing interests

All authors are affiliated with ImmuVia Inc. IMV-M is currently under development at ImmuVia Inc. as a potential oncology drug candidate.

Additional information

Supplementary Information The online version contains supplementary material available at https://doi.org/10.1038/s41598-025-93927-0.

Correspondence and requests for materials should be addressed to V.S.G.

Reprints and permissions information is available at www.nature.com/reprints.

Publisher's note Springer Nature remains neutral with regard to jurisdictional claims in published maps and institutional affiliations.